

Effect of Aromatic Additives with Various Alkyl Groups on Orientation Birefringence of Cellulose Acetate Propionate

Shogo Nobukawa,¹ Yoshihiko Aoki,¹ Hiroshi Yoshimura,² Yutaka Tachikawa,³ Masayuki Yamaguchi¹

¹Japan Advanced Institute of Science and Technology, 1-1 Asahidai, Nomi, Ishikawa 923-1292, Japan

²DIC Corporation, Chiba Plant, 12 Yawata-kaigandori, Ichihara, Chiba 290-8585, Japan

³DIC Corporation, Central Research Laboratories, 631 Sakado, Sakura, Chiba 285-8668, Japan

Correspondence to: S. Nobukawa (E-mail: nobukawa@jaist.ac.jp) or M. Yamaguchi (E-mail: m_yama@jaist.ac.jp)

ABSTRACT: Orientation birefringence and its wavelength dispersion in blends of cellulose acetate propionate (CAP) and aromatic additive molecules having various alkyl chains were investigated, in order to evaluate the effect of the chemical structure on the optical properties. We found that the additive improved the orientation birefringence of CAP, meaning that the additive orientation is parallel to CAP chains via the “nematic interaction (NI)” reflecting the intermolecular orientation correlation. The NI strength was evaluated by using a theory concerning the molecular orientation. The result demonstrates that the alkyl chain length in the additive molecule strongly affects the orientation correlation. Although the intrinsic birefringence monotonically decreases with the alkyl chain length, the NI strength shows the highest value between the additive with propionyl group and CAP. From the result, the contribution of birefringence from the aromatic molecule, which is determined by the intrinsic birefringence and orientation function, needs to be considered to design the optical films with high performances. © 2013 Wiley Periodicals, Inc. *J. Appl. Polym. Sci.* 130: 3465–3472, 2013

KEYWORDS: optical properties; cellulose and other wood products; films; plasticizer; rheology

Received 3 April 2013; accepted 31 May 2013; Published online 23 June 2013

DOI: 10.1002/app.39609

INTRODUCTION

For optical applications to liquid crystal and organic electro luminescence displays, birefringence is one of the most important optical properties. When a polymer film is uniaxially drawn above a glass transition temperature (T_g), an orientation birefringence, Δn , is induced as well as a stress, σ , due to the chain orientation.¹ Δn is represented by the difference between two refractive indices, $n_{||}$ and n_{\perp} in the directions parallel and perpendicular to the stretching direction.

$$\Delta n = n_{||} - n_{\perp} \quad (1)$$

For most of amorphous polymers, σ is proportional to Δn since both properties are associated with the orientation of the chain segment.¹

$$\Delta n = C\sigma \quad (2)$$

Here, C is the stress-optical coefficient, which is determined from repeating units of polymers. This relation is called the stress-optical rule (SOR). Since Δn is related to polarizability anisotropy of the chain segment, general polymers having

aromatic groups such as polystyrene (PS) and polycarbonate show high values of Δn .

Cellulose derivatives are expected as the eco-friendly materials for the various applications due to the biomass resources.^{2–11} Particularly, cellulose esters have been studied so far for the application to optical films due to their alternative properties such as heat resistance and transparency.^{10–15} Retardation films, which are one of optical films, have to be improved for the optical devices such as stereo (3D) and organic electro-luminescence (EL) displays since thin films is required for the weight saving of optical devices.^{15,16} Especially, the retardation film with less than 50 μm has been desired as a quarter wave-plate, so that its birefringence should be improved to at least 5×10^{-3} at 400 nm of wavelength. In order to produce the optical films with high performances, various techniques such as blending with other polymers^{17,18} or small molecules,^{19–21} copolymerization,^{22–24} and sheet piling²⁵ have been studied. Among these techniques, the addition of small molecules is relatively easier due to good miscibility with polymers than the others: for the polymer blending and copolymerization, the combination of species is limited. For the lamination, the

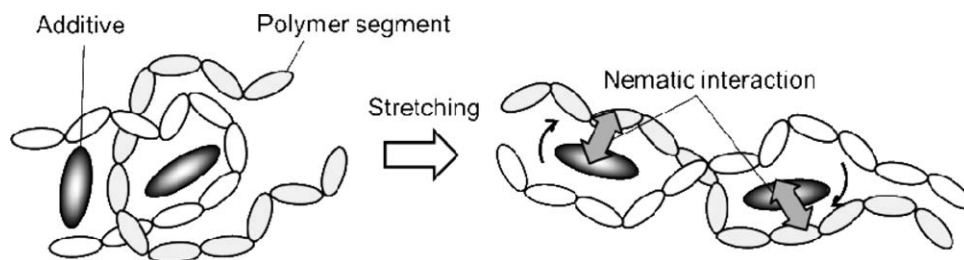


Figure 1. Schematic representation of orientation correlation between additive molecule and polymer chains. The additive orients along the main chain of the matrix polymer due to a NI associated with the orientation correlation.

thermal expansion mismatch between polymer sheets restricts the temperature range of use.

By using the model of the statistical segment approach²⁶, the orientation birefringence Δn is given as,

$$\Delta n = \frac{2\pi(n+2)^2 \rho N_A}{9n M_{\text{seg}}} \Delta\alpha \left[\frac{3\langle \cos^2\theta \rangle - 1}{2} \right] \quad (3)$$

Here, n , ρ , and N_A are refractive index, density, and Avogadro's number. M_{seg} and $\Delta\alpha$ are molecular weight and polarizability anisotropy of chain segment for the oriented polymers, and θ is the average angle between the segment and stretching direction. Therefore, as predicted by eq. (3), Δn can be improved by increasing the polarizability anisotropy of the polymers, such as, by introducing aromatic group.

Tagaya et al.¹⁹ reported that a small amount of rod-like molecules having large electric polarizability anisotropy can deny the negative Δn of poly(methyl methacrylate) (PMMA). According to them, Δn is controlled by only the concentration of the anisotropic molecules in the PMMA matrix. Abd Manaf et al.²¹ also found that tricresyl phosphate (TCP) improves Δn of cellulose ester films. These results suggest that the rod-like molecule and TCP orient parallel to the chain segments of matrix polymers due to the intermolecular orientation coupling which is called as the nematic interaction (NI) by Doi et al.²⁷

Since the NI works between intra-molecules (polymer segments or additive) and inter-molecules (polymer segment-additive) in the blends as represented in Figure 1, molecular orientation of the components affects each other. Nobukawa et al.^{16,28} investigated the intrinsic birefringence, Δn^0 , which is Δn for perfectly oriented polymers and reflects the polarizability anisotropy, in PS/aromatic additive blends by using the NI theory, and evaluated the orientation coupling. They also found that the long axis of the additive strengthens the intermolecular NI in the blends. However, this conclusion disagrees with the result of Tagaya et al., because the birefringence is determined by only Δn^0 . According to Doi et al. and Nobukawa et al., Δn in blends of polymers or polymer/additive is associated with intra- and inter-molecular NIs as well as the intrinsic birefringence reflecting the polarizability anisotropy. Hence, in order to improve Δn of CAP by using additive molecules, the effect of the chemical structure on the NI and Δn^0 has to be investigated. For this purpose, this article discusses the effect of the alkyl chain length of the aromatic compounds as the additives on Δn of CAP. Because the additives are oligomers composed of a repeating

unit, the molecular weight dependence on the two parameters is examined.

EXPERIMENTAL

Samples

Cellulose acetate propionate (CAP, Figure 2) used in this study was produced by Eastman Chemical Company (Kingsport, Tennessee). The weight-average and number-average molecular weights (M_w and M_n) of CAP were 2.1×10^5 and 7.7×10^4 , respectively, determined by a gel-permeation-chromatography (GPC, HLC-8020 Tosoh, Japan) with TSK-GEL[®] GMHXL using PS as a standard sample. Degrees of substitution for acetyl and propionyl groups per a pyranose unit of CAP are 0.19 and 2.58, respectively.

Seven types of aromatic compounds ($C_m\text{Ph}$, Figure 2) were synthesized from alkane diol and dimethyl terephthalate. The numbers of carbon in the alkyl chain (m) are 2, 3, 5, 6, and 9. The number-average molecular weight and the melting temperature of the additives are summarized in Table I. CAP and $C_m\text{Ph}$ with various weight ratios were mixed in a molten state by a 60 cc batch-type internal mixer (Labo-plastmil, Toyoseiki, Japan) at

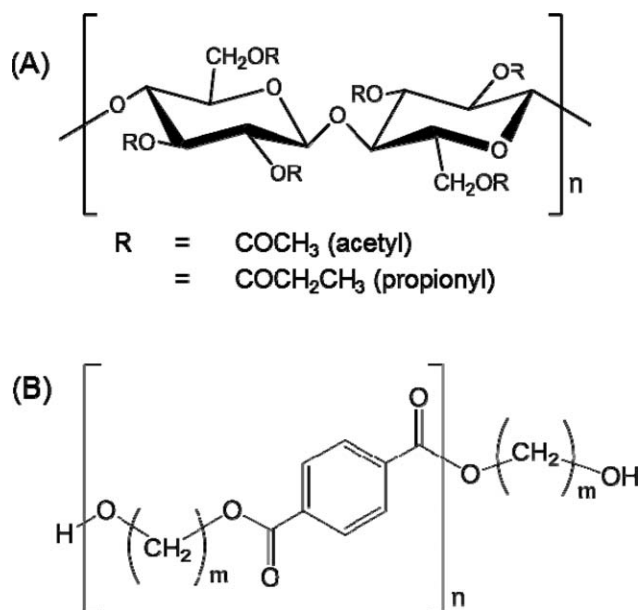


Figure 2. Chemical structures of (A) CAP and (B) aromatic ester compounds with various lengths of alkyl chain ($C_m\text{Ph}$).

Table I. Molecular Weight (M_n), Melting Point (T_m), and Intrinsic Birefringence (Δn^0) of Additives

Code	m^a	M_n^b	$T_m / ^\circ\text{C}^c$	Δn^0^d
C ₂ Ph	2	532	249	0.114
C ₂ Ph-L	2	477	243	0.114
C ₃ Ph	3	560	72	0.0837
C ₅ Ph	5	650	65	0.0673
C ₅ Ph-H	5	1129	101	0.0673
C ₆ Ph	6	720	68	0.0606
C ₉ Ph	9	860	71	0.0444

^aNumber of carbon atom in the alkyl group.

^bEstimated by GPC using standard polystyrene.

^cDetermined by DSC.

^dCalculated with molecular dynamics simulation.

200°C for 6 min. The blade rotation speed was 30 rpm. In order to prevent hydrolysis degradation and trans-esterification, CAP was dried *in vacuo* at 80°C for 2 h before the melt-mixing. After kept in vacuum oven at room temperature for one day, the blend samples were compressed to make sheets with a thickness of 200 μm at 200°C for 5 min under 10 MPa by a compression-molding machine (Table-type-test press SA-303-I-S, Tester Sangyo, Japan) and were subsequently cooled down at 25°C for 5 min.

Measurements

Dynamic mechanical analysis (DMA) for CAP/C_{*m*}Ph blend (100/10 wt/wt) films was performed to measure tensile storage and loss moduli (E' and E'' , respectively) at 10 Hz as a function of temperature by using a tensile oscillatory rheometer (DVE-E4000, UBM, Japan) from 25 to 180°C with a heating rate of 2 °C min⁻¹. A hot-stretching test for the films was carried out with various strain rates from 0.01 to 0.1 s⁻¹ by using a tensile drawing machine (DVE-3, UBM, Japan). The stretching temperature was determined from the DMA data, where the tensile modulus is 10 MPa at 10 Hz. The films were immediately quenched by cold air blowing after stretching to avoid relaxation of molecular orientation. The stretched samples were kept in a humidic chamber (IG420, Yamato, Japan) at 25°C and 50% RH for one day in order to ignore the moisture effect on the optical properties as previously reported.²⁹ The birefringence of the drawn films was measured as a function of wavelength by using an optical birefringence analyzer (KOBRA-WPR, Oji Scientific Instruments, Japan). The details of the optical system are explained in other paper.¹⁵

RESULTS AND DISCUSSION

Effect of Additives on Dynamic Mechanical Property of CAP

Figure 3(A,B) shows temperature dependence of dynamic tensile modulus at 10 Hz for CAP and CAP/additive blends. In Figure 3(A), the storage modulus E' of the blends started to decrease from lower temperature than that of CAP. The result suggests that the additives act as a plasticizer for CAP, since the drop of E' reflects the glass-to-rubber transition. In this study, a glass transition temperature (T_g) of the samples is

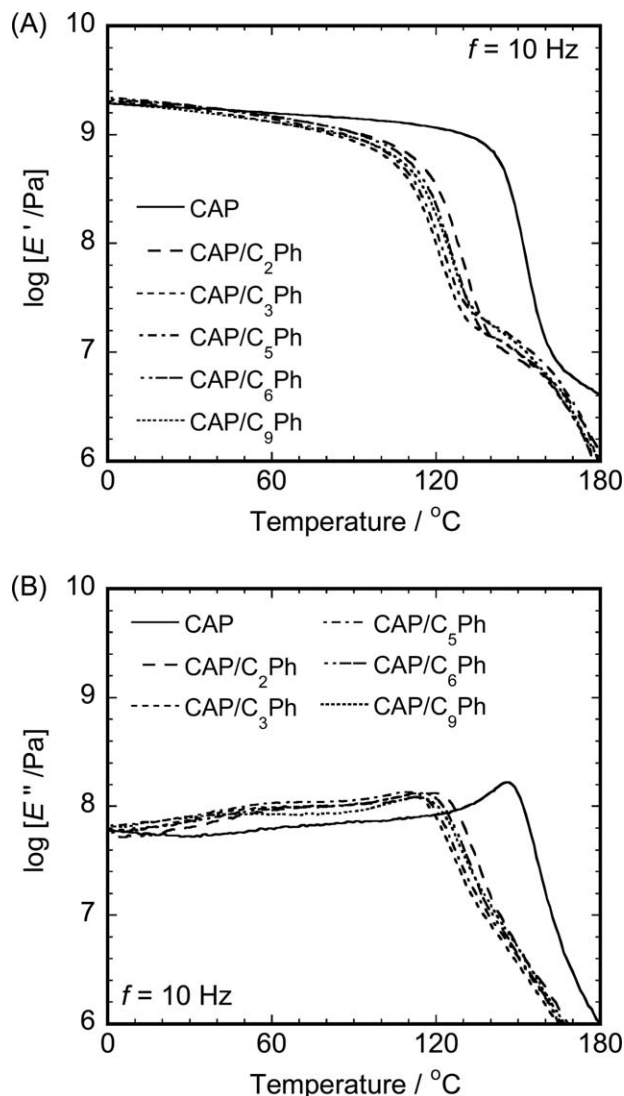


Figure 3. Temperature dependence of tensile (A) storage and (B) loss moduli (E' and E'') for bulk CAP, and CAP/additive blends with the weight ratio of 100/10 wt/wt. The oscillatory frequency is 10 Hz and heating rate is 2 °C min⁻¹.

defined as a peak temperature of loss modulus E'' , shown in Figure 3(B), which corresponds to α relaxation. The results summarized in Table II represent that degrees of the plasticization by the additives are similar although the melting points are not same as shown in Table I. Moreover, the α peak of E'' for the blends is wider than that for CAP, representing that the distribution of relaxation times for CAP becomes broader by addition of C_{*m*}Ph.

In Figure 3(B), the secondary β relaxation in all systems is also observed around 60°C. For cellulose acetate, β relaxation is observed near the room temperature and is assigned as local motion of small structural units.³⁰ The intensity of β relaxation peak increases by the additives while the peak position shifts to lower temperature. The results indicate that the additives having a large free volume activate the local motion including a wobbling or twisting fluctuation of pyranose units

Table II. Glass Transition Temperature (T_g) and Drawing Temperature (T_{draw}) for CAP and CAP/Additive Blends with a Weight Ratio of 100/10

Additive	T_g^a	$T_{\text{draw}} (^{\circ}\text{C})^b$	
		$E' = 10 \text{ MPa}$	100 MPa
-	146	163	152
C ₂ Ph	119	148	127
C ₂ Ph-L	116	148	125
C ₃ Ph	110	150	127
C ₅ Ph	110	151	127
C ₅ Ph-H	116	153	133
C ₆ Ph	114	152	128
C ₉ Ph	114	155	132

^aDefined to be a peak temperature of E'' in DMA data.

^bDetermined when E' is 10 or 100 MPa.

in CAP. This is reasonable as follows. In general, the small additives plasticize the glassy polymers with increasing the free volume related to the segmental motion. With increasing the free volume, the amplitude of the local motion for β relaxation becomes larger. However, we think that the segment structure reflecting the birefringence does not change by the additives because the uniaxial tensile test was carried out above T_g where the β relaxation completes.

In general, miscibility in polymer blends can be qualitatively discussed from the dynamic mechanical property as shown in Figure 3(A,B). No extra peak except α and β relaxations is observed in the figures, resulting that the additives, $C_m\text{Ph}$, in this experiment is well mixed with CAP matrix on the molecular level owing to the lower molecular weight.

Orientation Birefringence vs. Additive Compounds

A tensile strain induces the orientation of polymer chains and consequently the orientation birefringence, Δn , is generated. By using the Hermans orientation function of the chain, F , which represents the degree of orientation, Δn is given by,

$$\Delta n = \Delta n^0 F \quad (4)$$

where Δn^0 is an intrinsic birefringence which is determined by a polarizability anisotropy in the repeating unit.³¹

The additives in the blends are not responsible for the stress because of the low molecular weight. In contrast, the additive orientation can contribute to Δn of the blends. Therefore, eq. (2) is modified as follows,

$$\sigma_{\text{blend}} = \sigma_{\text{CAP}} \quad (5)$$

$$\begin{aligned} \Delta n_{\text{blend}} &= \Delta n_{\text{CAP}} + \Delta n_{\text{add}} \\ &= C_{\text{CAP}} \sigma_{\text{CAP}} + \Delta n_{\text{add}} \end{aligned} \quad (6)$$

Assuming that the stress-optical coefficient for CAP, C_{CAP} , does not change by the additives, Δn_{CAP} in the blends will be the same with that in the bulk when the same level of σ is obtained.

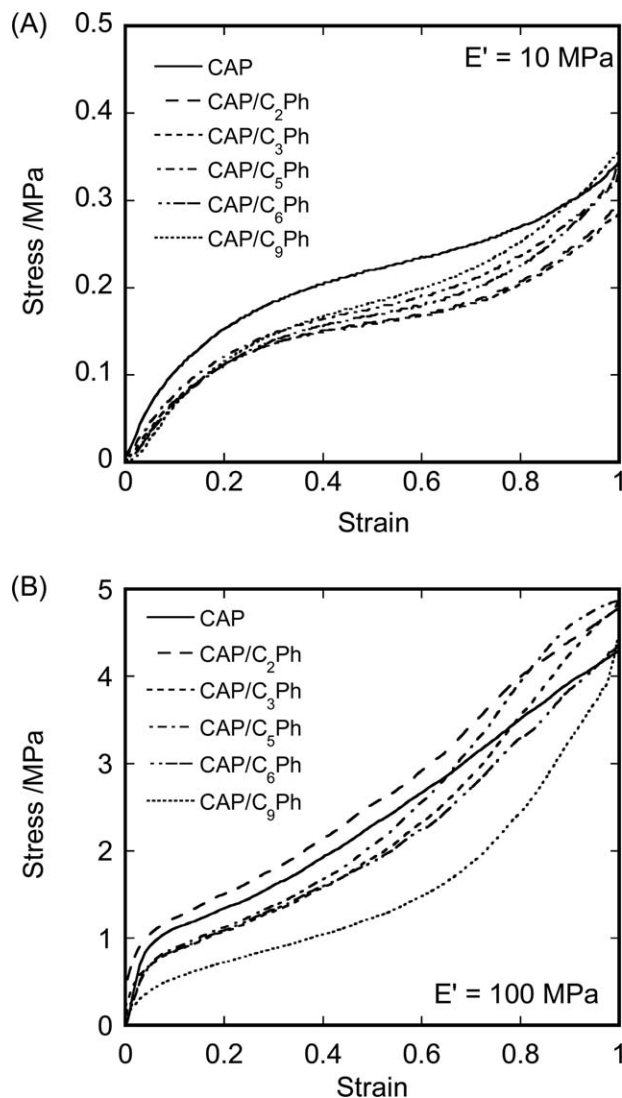


Figure 4. Stress–strain curves with the initial draw rate of 0.05 s^{-1} for CAP and CAP/additive blends (100/10 wt/wt) at two draw temperatures where E' are 10 and 100 MPa.

According to the Boltzmann superposition principle, the tensile stress at time t during a uniaxial drawing, $\sigma(t)$ is given by eq. (7).

$$\sigma(t) = \int_{-\infty}^t E(t-s) \dot{\epsilon}(s) ds \quad (7)$$

Here, E is Young's relaxation modulus and $\dot{\epsilon}$ is a tensile strain rate. When the same strain is applied, viscoelastic materials having the same value of Young's modulus will show a similar stress, that is, the same degree of orientation function of the matrix polymer. Following this idea, the drawing temperature (T_{draw}) was chosen at which the tensile storage modulus, E' , is 10 or 100 MPa in Figure 3(A). The values of T_{draw} are shown in Table II.

Figure 4(A,B) shows stress–strain curves of the CAP and CAP blend films with an engineering strain rate of 0.05 s^{-1} . The stress in each figure is almost same for all samples, suggesting that the chain orientation of CAP, F_{CAP} , can be regarded to be

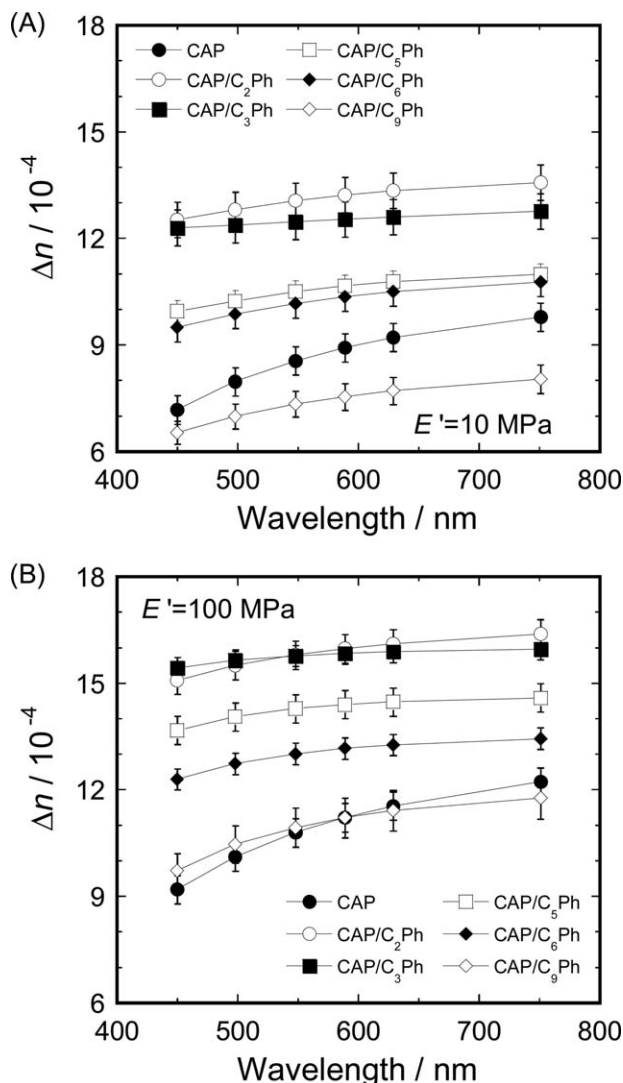


Figure 5. Wavelength dependence of orientation birefringence for CAP and CAP/additive blends (100/10 wt/wt) drawn at two temperature where E' is 10 and 100 MPa.

similar as predicted from eqs. (2) and (3). The tensile test at the high T_{draw} ($E' = 10$ MPa) exhibits the rubber-like stress-strain behavior without yield point. On the other hand, the tensile test at the low T_{draw} ($E' = 100$ MPa) shows the yield behavior due to the presence of glassy stress. According to Inoue et al.,³² the SOR is not applicable for the tensile stretching near T_g because the glassy stress having the different C should be considered to Δn .

Wavelength dispersions of Δn for CAP and the blends at two T_{draw} are shown in Figure 5. CAP has positive birefringence and extraordinary wavelength dispersion: birefringence increases with wavelength. General polymers show the ordinary dispersion, that is, the birefringence decreases with the wavelength. Yamaguchi et al.¹⁵ concluded that the extraordinary wavelength dispersion is originated from the contributions of two ester groups in CAP. In Figure 5, at both stress levels, the stretched films of CAP/ C_m Ph blends excepting C_9 Ph represent higher Δn than that of CAP. The reduction of Δn in CAP/ C_9 Ph blend is

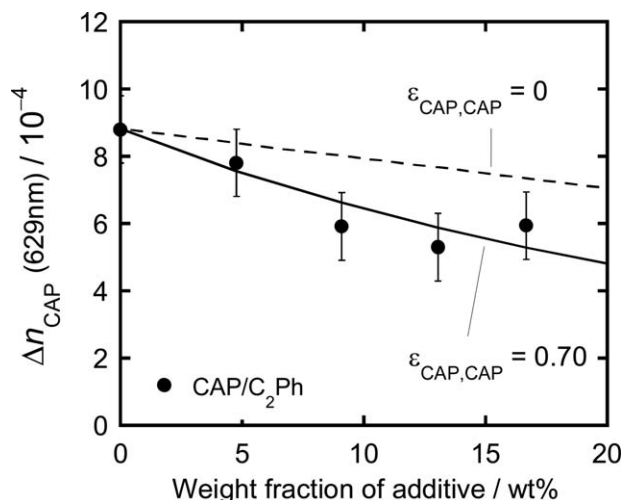


Figure 6. Birefringence of CAP in blends with C_2 Ph at various weight fractions. The broken and solid lines represent the calculated results from the NI theory in eq. (8) with $\epsilon_{\text{CAP,CAP}} = 0$ and 0.7, respectively.

due to the intramolecular orientation correlation of CAP chains as discussed in next section. Furthermore, the wavelength dependence becomes weaker in the presence of the additives. Since the additive molecules show the ordinary dispersion of positive birefringence, the change in the wavelength dependence suggests the additive orientation cooperative with the CAP chain during the stretching.

Orientation Birefringence and Nematic Interaction in Various Lengths of Additives

The molecular orientation of C_m Ph additive enhancing Δn is due to the NI with CAP chain. The orientation birefringence of the additives, Δn_{add} , can be evaluated by using following equations based on the NI theory.²⁸

$$\begin{aligned} \Delta n_{\text{blend}} &= \Delta n_{\text{CAP}} + \Delta n_{\text{add}} \\ &= \left[\frac{\Delta n_{\text{CAP}}^0 (1 - \epsilon_{\text{CAP,CAP}})}{1 - \varphi_{\text{CAP}} \epsilon_{\text{CAP,CAP}}} \right] \varphi_{\text{CAP}} F_{\text{CAP}} + \Delta n_{\text{add}} \end{aligned} \quad (8)$$

$$\sigma = \sigma_{\text{CAP}} \propto \varphi_{\text{CAP}} F_{\text{CAP}} \quad (9)$$

Here, $\epsilon_{i,j}$ is a NI parameter representing orientational correlation of component i in the orientation field of component j and it takes from -0.5 to 1. The parameter φ is the volume fraction. In eq. (8), $\varphi_{\text{CAP}} F_{\text{CAP}}$ in the blends is almost the same with that in the bulk because the tensile stresses are comparable.

In order to evaluate the NI strength in the blends, we assumed that the wavelength dispersions of component birefringence, Δn_{CAP} and Δn_{add} , are not changed by blending. This assumption will be applicable because the wavelength dispersion is determined by the absorption wavelength reflecting the chemical structure.¹⁵ As a result, Δn of the blends was separated into Δn_{CAP} and Δn_{add} . Figure 6 shows Δn_{CAP} at various compositions in CAP/ C_2 Ph as an example. Δn_{CAP} decreases with increasing the weight fraction of additives, meaning that the total birefringence of the blend will decrease without the additive birefringence. For instance, Δn of CAP/ C_9 Ph is lower than

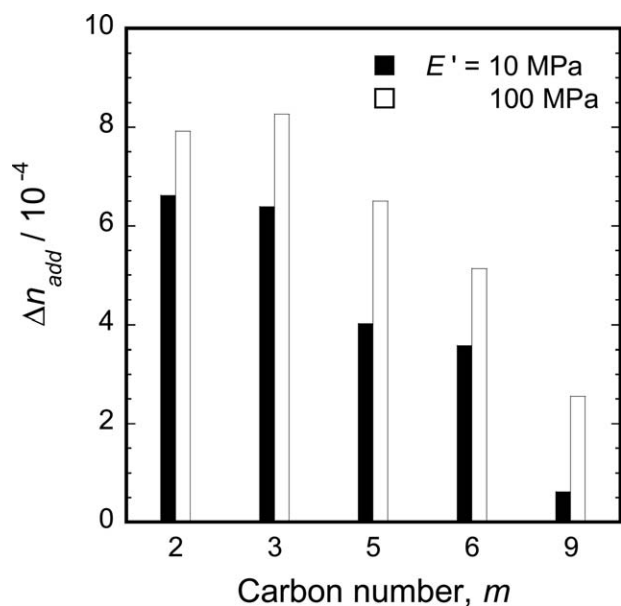


Figure 7. Comparison of orientation birefringence for additives in blend films after stretching with a draw ratio of 2.0 at two temperatures.

that of bulk CAP in Figure 5(A), suggesting that Δn_{add} of $C_9\text{Ph}$ is negligibly small.

The relationship for CAP component in eq. (8) evaluates the NI strength between CAP–CAP from the Δn_{CAP} data. When the NI between CAP chains is negligible, Δn_{CAP} is estimated as dotted line as shown in the figure by using eq. (8). The value evaluates the NI strength between CAP chains, $\varepsilon_{\text{CAP,CAP}}$ to be 0.7 as represented by the solid line. By comparing the dotted and solid lines and by applying the $\varepsilon_{\text{CAP,CAP}}$ value to eq. (8), Δn_{add} was estimated as shown in Figure 7. At both temperatures, Δn_{add} decreases with the carbon number of alkyl chain. This order qualitatively corresponds to the intrinsic birefringence of the additives in Table I. According to the NI theory, Δn_{add} is determined by the NI parameters as represented by,

$$\begin{aligned} \Delta n_{\text{add}} &= \Delta n_{\text{add}}^0 \varphi_{\text{add}} F_{\text{add}} \\ &= \Delta n_{\text{add}}^0 \varphi_{\text{add}} \left[\frac{\varphi_{\text{CAP}} \varepsilon_{\text{CAP,add}}}{1 - \varphi_{\text{CAP}} \varepsilon_{\text{CAP,CAP}}} \right] F_{\text{CAP}} \end{aligned} \quad (10)$$

Since $\varepsilon_{\text{CAP,CAP}}$ is independent on the additive species, $F_{\text{add}}/F_{\text{CAP}}$ reflects the intermolecular NI strength, $\varepsilon_{\text{CAP,add}}$. As shown in Figure 4, the tensile stresses in the blends were in the same level, indicating that F_{CAP} will be comparable. Therefore, the comparison of $\varepsilon_{\text{CAP,add}}$ in the blends can be replaced to that of F_{add} , which is calculated by eq. (3) as represented in Figure 8. Unlike Δn_{add} in Figure 7, F_{add} does not show the m dependence excepting $m = 9$, suggesting that, in the short length range of alkyl group, i.e., $2 \leq m \leq 6$, the orientation coupling in the blends, $\varepsilon_{\text{CAP,add}}$, is not strongly dependent on m for the additives. However, for $m \geq 6$, $\varepsilon_{\text{CAP,add}}$ become smaller, especially at high T_{draw} where E' is 10 MPa. Nobukawa et al.^{16,28} found that the orientation coupling of rod-like molecules with matrix

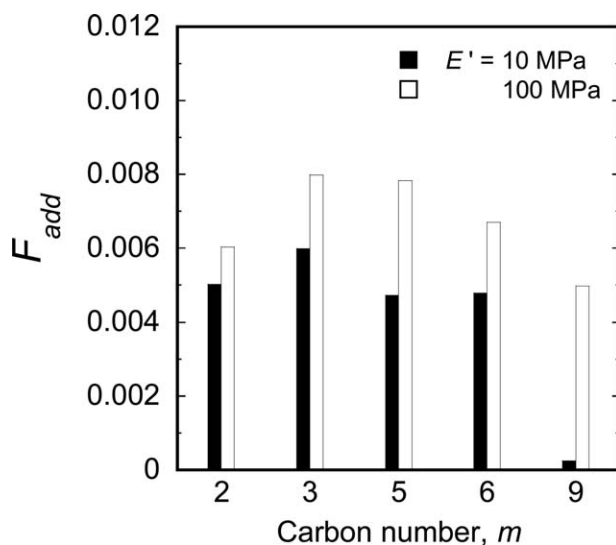


Figure 8. Orientation function (F) of additives in blend films after stretching with a draw ratio of 2.0 at two temperatures.

polymers is affected by the chemical structure and the molecular size/shape reflecting the flexibility. In Figure 8, the similar result of $\varepsilon_{\text{CAP,add}}$ at high T_{draw} was observed owing to the larger flexibility of $C_m\text{Ph}$ having the longer alkyl chain.

$\varepsilon_{\text{CAP,add}}$ in the blends at low T_{draw} is observed to be larger than that at high T_{draw} . Abd Manaf et al.²¹ found that the orientation relaxation of the aromatic plasticizer dissolved in CAP after hot-stretching of the blend films by using simultaneously the stress and birefringence relaxation measurements. By utilizing a time–temperature-superposition principle, the lower T_{draw} has the same meaning with the shorter time where the orientation does not relax so much. For this reason, the orientation of $C_m\text{Ph}$ at low T_{draw} is stronger than that at high T_{draw} . In particular, the orientation relaxation of $C_9\text{Ph}$ almost completes at high T_{draw} indicating that the intermolecular NI does not exist in the CAP/ $C_9\text{Ph}$ blend.

Molecular Weight Dependence on the Nematic Interaction

Actually, the additive molecules used in this study have the wide distribution of molecular weight owing to the condensation reaction of alkane diol and dimethyl terephthalate. In order to discuss the molecular weight dependence on the orientation coupling in CAP/ $C_m\text{Ph}$ blends, the wavelength dispersion of Δn for two blends with $m = 2$ and 5 are shown in Figures 9 and 10. The drawing temperature with high T_{draw} was chosen to avoid the contribution of the glassy stress to the orientation birefringence as observed at low T_{draw} . The effect of $C_2\text{Ph}$ and $C_2\text{Ph-L}$ with lower molecular weight on Δn is compared within the experimental error in Figure 9. The wavelength dispersions of Δn in both blends are comparable at the low and high T_{draw} 's, meaning that the difference in molecular weight of the additive lower than about 600 g mol^{-1} does not affect the intermolecular NI with CAP.

Contrary, the effects of $C_5\text{Ph}$ and $C_5\text{Ph-H}$ on Δn are compared in Figure 10. The wavelength dependences of Δn in both blends are likely similar while Δn with $C_5\text{Ph-H}$ is obviously larger than

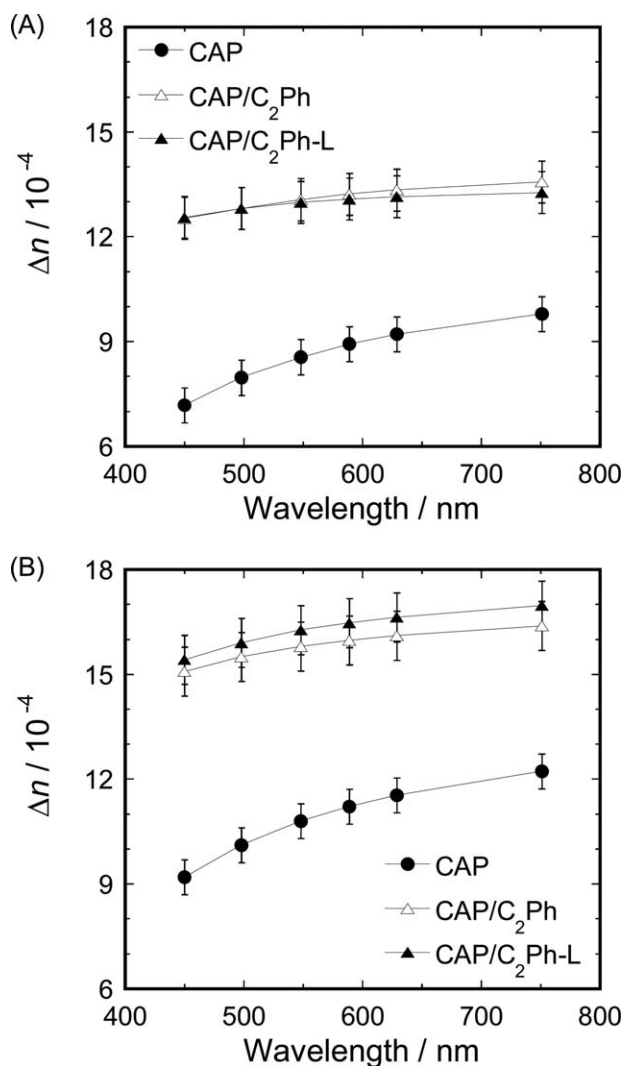


Figure 9. Wavelength dependence of orientation birefringence for CAP and CAP/C₂Ph blends drawn at two temperatures where E' is 10 and 100 MPa.

that with C₅Ph, representing that C₅Ph-H shows the higher orientation parallel to CAP chain. C₅Ph-H exhibits the slow orientation relaxation than C₅Ph due to the higher molecular weight. Hence, the higher Δn in CAP/C₅Ph-H blend is due to the difference in the relaxation time, meaning that the intermolecular NI strength is independent of the molecular weight.

CONCLUSIONS

The effect of alkyl chain length of the aromatic additive, alkyl terephthalate oligomer (C_mPh), on the orientation birefringence of CAP was examined by measuring the stress and the orientation birefringence. The birefringence was enhanced by the presence of C_mPh, indicating that the parallel orientation of C_mPh to CAP chain took place. Based on the NI theory previously introduced, the orientation degree of C_mPh in the blends was estimated from the birefringence data. From the results it was found that the NI strength of C_mPh with matrix CAP increases with decreasing the number of carbon, m , in alkyl chain. Particularly, when m is larger than 6, the NI disappeared.

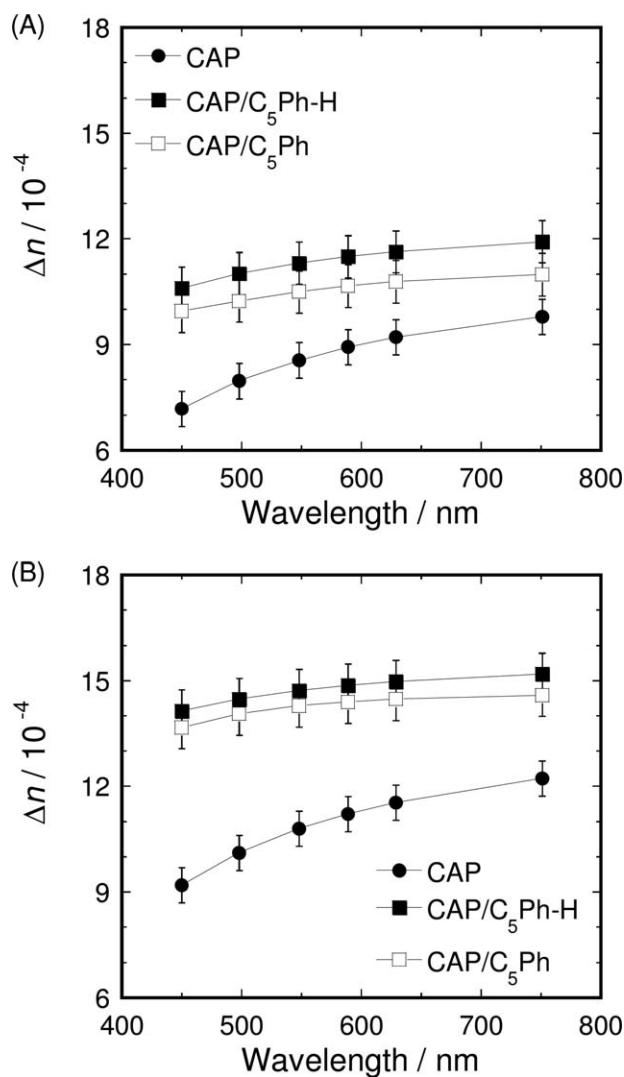


Figure 10. Wavelength dependence of orientation birefringence for CAP and CAP/C₅Ph blends drawn at two temperatures where E' is 10 and 100 MPa.

The orientation birefringence in the blends of CAP and C_mPh having different molecular weights was investigated. The result represented that the higher molecular weight slightly enhanced the orientation birefringence in the blends due to the slow relaxation of the C_mPh with higher molecular weight. However, we think that the intermolecular NI between C_mPh and CAP is independent on the molecular weight studied in this article.

From the obtained results above, in order to enhance the orientation birefringence, the aromatic molecules having the shorter alkyl chain and higher molecular weight are better because of the stronger NI strength and the slow relaxation time.

ACKNOWLEDGMENTS

This work was partly supported by Research Activity Start-up from the Japan Society for the Promotion of Science (23850008), and by grant from the Ogasawara Foundation for the Promotion of Science and Engineering.

REFERENCES

1. Doi, M.; Edwards, S. F. *The Theory of Polymer Dynamics*; Oxford University Press: New York, **1986**.
2. Edgar, K. J.; Buchanan, C. M.; Debenham, J. S.; Rundquist, P. A.; Seiler, B. D.; Shelton, M. C.; Tindall, D. *Prog. Polym. Sci.* **2001**, *26*, 1605.
3. Kono, H.; Numata, Y.; Erata, T.; Takai, M. *Polymer* **2004**, *45*, 2843.
4. Sikorski, P.; Wada, M.; Heux, L.; Shintani, H.; Stokke, B. T. *Macromolecules* **2004**, *37*, 4547.
5. Kondo, T.; Sawatari, C.; Manley, R. S.; Gray, D. G. *Macromolecules* **1994**, *27*, 210.
6. Kondo, T.; Sawatari, C. *Polymer* **1996**, *37*, 393.
7. Krasovskii, A. N.; Plodisty, A. B.; Polyakov, D. N. *Russ. J. Appl. Chem.* **1996**, *69*, 1048.
8. Heinze, T.; Dicke, R.; Koschella, A.; Kull, A. H.; Klohr, E. A.; Koch, W. *Macromol. Chem. Phys.* **2000**, *201*, 627.
9. Maeda, A.; Inoue, T. *Nihon Reorji Gakkaishi* **2011**, *39*, 159.
10. Sata, H.; Murayama, M.; Shimamoto, S. In MGAMA Workshop, Heidelberg, Germany, 29 September to 1 October, 2003, **2004**; p 323.
11. Yamaguchi, M.; Abd Manaf, M. E.; Songsurang, K.; Nobukawa, S. *Cellulose* **2012**, *19*, 601.
12. Ilharco, L. M.; de Barros, R. B. *Langmuir* **2000**, *16*, 9331.
13. Songsurang, K.; Miyagawa, A.; Abd Manaf, M. E.; Phulkerd, P.; Nobukawa, S.; Yamaguchi, M. *Cellulose* **2012**, *20*, 83.
14. Hishikawa, Y.; Togawa, E.; Kondo, T. *Cellulose* **2010**, *17*, 539.
15. Yamaguchi, M.; Okada, K.; Edeerozey, M.; Shiroyama, Y.; Iwasaki, T.; Okamoto, K. *Macromolecules* **2009**, *42*, 9034.
16. Nobukawa, S. Doctoral Thesis, Osaka University, Toyonaka, **2011**.
17. Saito, H.; Inoue, T. *J. Polym. Sci. Part B: Polym. Phys.* **1987**, *25*, 1629.
18. Uchiyama, A.; Yatabe, T. *Jpn. J. App. Phys. Part 1* **2003**, *42*, 3503.
19. Tagaya, A.; Iwata, S.; Kawanami, E.; Tsukahara, H.; Koike, Y. *App. Opt.* **2001**, *40*, 3677.
20. Tagaya, A.; Ohkita, H.; Harada, T.; Ishibashi, K.; Koike, Y. *Macromolecules* **2006**, *39*, 3019.
21. Abd Manaf, M. E.; Tsuji, M.; Shiroyama, Y.; Yamaguchi, M. *Macromolecules* **2011**, *44*, 3942.
22. Iwasaki, S.; Satoh, Z.; Shafiee, H.; Tagaya, A.; Koike, Y. *Polymer* **2012**, *53*, 3287.
23. Uchiyama, A.; Ono, Y.; Ikeda, Y.; Shuto, H.; Yahata, K. *Polym. J.* **2012**, *44*, 995.
24. Cimrova, V.; Neher, D.; Kostromine, S.; Bieringer, T. *Macromolecules* **1999**, *32*, 8496.
25. Cho, C. K.; Kim, J. D.; Cho, K.; Park, C. E.; Lee, S. W.; Ree, M. *J. Adhes. Sci. Technol.* **2000**, *14*, 1131.
26. Wilkes, G. L.; Stein, R. S. In *Structure and Properties of Oriented Polymers*; Ward, I. M., Ed.; Chapman & Hall: London, **1997**; pp. 44–141.
27. Doi, M.; Pearson, D.; Kornfield, J.; Fuller, G. *Macromolecules* **1989**, *22*, 1488.
28. Nobukawa, S.; Urakawa, O.; Shikata, T.; Inoue, T. *Macromolecules* **2010**, *43*, 6099.
29. Abd Manaf, M. E.; Tsuji, M.; Nobukawa, S.; Yamaguchi, M. *Polymers* **2011**, *3*, 955.
30. Videki, B.; Klebert, S.; Pukanszky, B. *J. Polym. Sci. Part B: Polym. Phys.* **2007**, *45*, 873.
31. Hermans, P. H.; Platzek, P. *Kolloid Z.* **1939**, *88*, 68.
32. Inoue, T.; Ryu, D. S.; Osaki, K. *Macromolecules* **1998**, *31*, 6977.